

Pathological role of Toll-like receptor signaling in cerebral malaria

Cevayir Coban^{1,2*}, Ken J. Ishii^{1,3*}, Satoshi Uematsu¹, Nobuko Arisue⁴, Shintaro Sato^{1,3}, Masahiro Yamamoto¹, Taro Kawai^{1,3}, Osamu Takeuchi^{1,3}, Hajime Hiseada⁵, Toshihiro Horii⁴ and Shizuo Akira^{1,2,3}

¹Department of Host Defense, Research Institute for Microbial Diseases, ²21st Century Center of Excellence, Combined Program on Microbiology and Immunology, ³Exploratory Research for Advanced Technology, Japan Science and Technology Agency and ⁴Department of Molecular Protozoology, Research Institute for Microbial Diseases, Osaka University, Suita, Osaka 565-0871, Japan

⁵Department of Parasitology, Graduate School of Medical Sciences, Kyushu University, Fukuoka 812-8582, Japan

Keywords: cell trafficking, hemozoin, innate immunity, MyD88, *Plasmodium*

Abstract

Toll-like receptors (TLRs) recognize malaria parasites or their metabolites; however, their physiological roles in malaria infection *in vivo* are not fully understood. Here, we show that myeloid differentiation primary response gene 88 (MyD88)-dependent TLR signaling mediates brain pathogenesis of severe malaria infection, namely cerebral malaria (CM). A significant number of MyD88-, but not TIR domain containing adaptor-inducing IFN-beta (TRIF)-deficient or wild-type (WT) mice survived CM caused by *Plasmodium berghei* ANKA (PbA) infection. Although systemic parasitemia was comparable, sequestration of parasite and hemozoin load in the brain blood vessels was significantly lower in MyD88-deficient mice compared with those in TRIF-deficient or WT mice. Moreover, brain-specific pathological changes were associated with MyD88-dependent infiltration of CD8⁺, CCR5⁺ T cells and CD11c⁺ dendritic cells, including CD11c⁺, NK1.1⁺ and B220⁺ cells, and up-regulation of genes such as *Granzyme B*, *Lipocalin 2*, *Ccl3* and *Ccr5*. Further studies using mice lacking various TLRs suggest that TLR2 and TLR9, but not TLR4, 5 and 7, were involved in CM. These results strongly suggest that TLR2- and/or TLR9-mediated, MyD88-dependent brain pathogenesis may play a critical role in CM, the lethal complication during PbA infection.

Introduction

Cerebral malaria (CM) is the lethal complication of malaria caused by *Plasmodium falciparum* in humans. Besides the high mortality rates, persistent neurocognitive deficits after recovery have become an increasing concern in past decades (1–3). While precise molecular and cellular mechanisms underlying the pathogenesis of CM are not yet fully elucidated, *Plasmodium berghei* ANKA (PbA) infection in mice provides valuable information as an experimental model of CM (4–6). After infection with PbA, susceptible mice (e.g. C57Bl/6) develop symptoms within a week, such as ataxia, hemi- or paraplegia, seizures and coma, and die within the following 24 h. Profound intravascular changes occur in cerebral vessels, such as endothelial cell damage and sequestration of infected erythrocytes, as well as host immune cells (i.e. platelets and leukocytes).

In recent decades, host immune responses to parasites have been implicated in playing an important role in CM pathogenesis. For example: (i) systemic pro-inflammatory cytokines such as IL-12, IFN γ and tumor necrosis factor (TNF) α , but not IL-1 or IL-18 (7–9); and (ii) specific cell types, such as CD1d-restricted NK T cells and CD8⁺ T cells (10, 11), have been reported as critical mediators in CM development. Immune cell trafficking through CCR5 but not CCR2 has been found to be critical for leukocyte accumulation in the brain of CM-susceptible mice (12). However, the precise mechanism by which innate immune receptors or their signaling triggers such brain as well as systemic inflammation and immune cell trafficking is not known.

Toll-like receptors (TLRs) have been identified as key host molecules in innate immune recognition of and response to

*These authors contributed equally to this study.

Correspondence to: S. Akira; E-mail: sakira@biken.osaka-u.ac.jp

Transmitting editor: K. Inaba

Received 23 August 2006, accepted 24 October 2006

Advance Access publication 29 November 2006

microbial products including lipids, proteins and nucleic acids (13). Recent evidence suggests that TLRs are involved in the innate immune responses to *Plasmodium* species (14). Adachi *et al.* (15) for the first time has analyzed the involvement of TLRs *in vivo* using a mouse malaria infection model where myeloid differentiation primary response gene 88 (MyD88), an essential adaptor molecule for most TLRs, is critical for IL-12 induction by *P. berghei* NK65 parasites, causing liver injury. Recently, glycosyl-phosphatidylinositol (GPI) and hemozoin (a parasite heme metabolite) derived from *P. falciparum* have been identified as the ligands for TLR2 and TLR9, respectively (16, 17), whereas other heat-labile molecules derived from the malaria parasite are still to be clarified for TLR9-mediated recognition (18).

Based on the above findings, we investigated the role of TLRs and their signaling molecules in the pathogenesis of CM. We used an *in vivo* experimental model for CM in which various mutant mice lacking TLRs and their adaptor molecules, such as MyD88 and TIR domain containing adaptor-inducing IFN- β (TRIF), were infected with PbA. Monitoring survival, CM symptoms, parasitemia, hemoglobin level, pathological changes in the brain and host immune responses after infection revealed that TLR2-, TLR9- and MyD88-dependent signaling, but not TLR4-, TLR5-, TLR7- or TRIF-dependent signaling, facilitated CM pathogenesis and its resultant mortality. Analysis of systemic, as well as local inflammatory responses, suggest that the TLR-MyD88-dependent CM pathogenesis was associated with not only systemic inflammatory responses but also with brain sequestration of parasite, as well as hemozoin, and infiltration of particular lymphocytes, such as CCR5⁺, CD8⁺ T cells and CD11c⁺ dendritic cells (DCs) including NK1.1⁺, B220⁺ and CD11c⁺ cells, expressing both DC and NK cell marker.

Methods

Animals

Mice deficient for MyD88, TRIF, TLR2, TLR4, TLR5, TLR7 or TLR9 were generated as described previously (19–25). Except TRIF^{−/−} mice and their littermate controls which are on a 129/Ola × C57Bl/6 (B6.129) background, all mice used here were backcrossed to C57Bl/6 (B6) background at least for eight generations. Age (6–10 weeks old)- and sex-matched groups of wild-type (WT) (either purchased from CLEA, Japan, or wild-type littermates) and knockout mice were used in the experiments. Animal experiments for infection were approved by the institutional protocol of the Research Institute for Microbial Diseases, Osaka University.

PbA infection and CM assessment

First, donor mice (either B6 or B6.129) were infected with the frozen stock of PbA-infected RBCs (iRBCs), and 6–7 days later, when the parasitemia showed mostly ring stages, and the mice suffered from CM symptoms, blood was drawn and used for infection studies. We chose this method to infect each mouse with similar blood-stage parasites. Then, WT or various mutant mice were infected with 10⁶ iRBCs intra-peritoneally in 200 μ l PBS. Parasitemia was assessed every 2 days by microscopy of Giemsa-stained thin blood

smears. Survival and signs of disease were monitored daily. Animals that showed neurological signs, such as convulsions, ataxia and paralysis, and died between 6 and 12 days after infection were considered as having CM. Brains were removed and used for histological analysis and reverse transcription (RT)-PCR. Serum was taken for cytokine ELISA and kept at −80°C until use. Blood hemoglobin levels were analyzed by using Drabkin's solution, as described elsewhere (12).

Cell culture, PbA crude extract and hemozoin

The murine microglial cell line BV-2 was cultured in 10% fetal bovine serum (FBS)-containing DMEM medium as described before (26). One million cells ml^{−1} were seeded on to a six-well culture plate and stimulated for 24 h as indicated. Then, cells were collected, and total RNA was extracted using TRIzol reagent. RT-PCR was performed as mentioned below. PbA crude extract was prepared from the blood of infected mice, as described elsewhere (27). Hemozoin was prepared from Mycoplasma-free *P. falciparum* cultures as described before (17). CpG ODN 1555 was used as a control stimulant (26).

Histology

Six days after PbA infection, brains were perfused with PBS and carefully removed and fixed in formaldehyde solution (4% v/v). Tissue sections were prepared and stained with hematoxylin and eosin (HE) as described elsewhere (10). The sections were also stained by Prussian blue in order to visualize and count the hemozoin clusters. After staining with potassium ferrocyanide, counterstaining with nuclear fast red solution allowed us to visualize dark brown hemozoin clusters that were easily counted by light microscopy (Fig. 2B).

Flow cytometry of brain-infiltrating lymphocytes

On day 6 after PbA infection, lymphocytes from brain were isolated as previously described (12). Briefly, after perfusion with PBS to remove the circulating blood cells, brains were crushed and washed in RPMI 1640 medium supplemented with 10% FBS and penicillin–streptomycin. Brain tissue extracts were then pelleted by centrifugation at 400 × *g* for 5 min, and were further purified on a 30% Percoll gradient (Amersham) (400 × *g* for 30 min). Cells were counted, fixed and stained with FITC-, PE-, CyChrome- or allophycocyanin (APC)-labeled antibody in the presence of anti-CD16 antibody for 30 min at room temperature, as previously described (17). Stained cells were washed, re-suspended in PBS/0.1% BSA/0.1% NaN₃ and analyzed by FACSCalibur, followed by analysis using CellQuest software (Becton Dickinson). All antibodies used were purchased from Becton Dickinson. T cell staining was performed using CD8-APC (or -FITC), Thy1.2-PE, TCR β -CyChrome, CD4-APC (or -FITC) and CCR5-PE. NK cells, B cells and DCs were stained with NK1.1-PE, CD45R (B220)-CyChrome and CD11c-APC (28, 29).

DNA microarray analysis

On day 6 of infection with PbA, half of the brain tissues were removed and kept at −80°C. Total RNA was extracted from individual brains with TRIzol and further purified by RNeasy

kit (Qiagen, Hilden, Germany), and cDNA was synthesized from total RNA with the SuperScript Choice System (Invitrogen, Carlsbad, CA, USA). These cDNAs were used to prepare biotin-labeled cRNA according to the manufacturer's protocol (Enzo Diagnostics, Farmingdale, NY, USA). Purification of cRNA and hybridization and scanning of the microarray were done according to the manufacturer's instructions (Affymetrix, MG U74A version 2). Data analysis was carried out by using a Suite software version 5.0 (Affymetrix) and GeneSpring software version 6.0 (SiliconGenetics, Redwood, CA, USA) (30). To confirm the gene changes, the experiment was performed twice by using two mice per group.

RT-PCR

RT-PCR was carried out as described elsewhere (30). Briefly, brain tissues were homogenized and total RNA was extracted with TRIzol reagent (Invitrogen) according to the manufacturer's protocol. Then, 1 µg total RNA was reverse transcribed with SuperScript II (Invitrogen). PCR amplification was performed using recombinant *Taq* DNA polymerase (Takara Shuzo). PCR conditions were 30 s denaturation at 94°C, 30 s annealing at 60°C and 1 min elongation at 72°C for 30 cycles. Specific primers used were as follows: *Granzyme B*, sense 5'-TCGACCCTACATGGCCTTAC-3' and anti-sense 5'-TGGGGAATGCATTTTACCAT-3'; *Lipocalin 2*, sense 5'-CCAGTTCGCATGGTATTTT-3' and anti-sense 5'-CACACTCACCACCCATT CAG-3'; *MIP-1α*, sense 5'-ATGAAGGTCTCCACCACTGCCC-AAGC-3' and anti-sense 5'-TTAGTCAGGAAATGACACCTG GCTGGG-3'; *IL-6*, sense 5'-GACAAAGCCAGAGTCCCTTCAG AGAG-3' and anti-sense 5'-CTAGGTTTGCCGAGTAGATCC TC-3' and β -actin, sense 5'-GACATGGAGAAGATCTGGCAC CACA-3' and anti-sense 5'-ATCTCCTGCTCGAAGTCTAGA-CAA-3'. Density of the PCR products in ethidium bromide-stained gel was measured by NIH image software (<http://rsb.info.nih.gov/ni-image/download.html>). Quantities of each transcript were compared with the β -actin reference.

ELISA

Mouse IFN γ , TNF α and IL-12p40 in the serum were measured by ELISA (DuoSet ELISA Kit, R&D Systems, Minneapolis, MN, USA) according to the manufacturer's instructions.

Statistical analysis

Differences between groups were analyzed for statistical significance by using SigmaStat 3.0 software with either Student's *t*-test or Mann–Whitney *U*-test. For survival curves, Kaplan–Meier plots and log rank tests were performed. *P* < 0.05 was considered statistically significant.

Results

Critical role of MyD88 in CM and its resultant lethality, but not in systemic parasitemia

MyD88 is an essential adaptor molecule for most TLR signaling, whereas TRIF is an indispensable adaptor for TLR3 and TLR4 (31). To examine the possible role of innate immune responses through TLRs in CM pathogenesis, we first infected intra-peritoneally MyD88- or TRIF-deficient mice with a C57Bl/6 (B6) or 129/Ola \times C57Bl/6 (B6.129) back-

ground, then monitored their survival, parasitemia, percentage hemoglobin in the blood. B6.129 mice were susceptible to CM with 10⁶ PbA and frequency of characteristic CM symptoms were consistent with a previous report (12). After infection, WT mice showed CM symptoms within 6–12 days and died within the following 24 h; however, a significant number of MyD88-deficient mice survived CM and eventually died of extremely high parasitemia, reaching >85% (Fig. 1A, *P* = 0.003 by log rank survival test). In sharp contrast, infected TRIF-deficient mice died even before the WT controls, during which all of the TRIF-deficient mice suffered from CM (Fig. 1B, *P* = 0.325 by log rank survival test). Overall survival from CM was significantly higher in MyD88-deficient mice than that in WT or TRIF-deficient mice [Fig. 1C and D, 10% of WT (*n* = 50) versus 46.15% of MyD88^{-/-} (*n* = 39) mice escaped from CM; 9.1% of WT (*n* = 16) versus none of the TRIF^{-/-} (*n* = 16) mice escaped from CM].

Systemic parasitemia and hemoglobin levels were comparable between WT and MyD88- and TRIF-deficient mice during the first week of PbA infection (Fig. 1A and B and data not shown), similar to a previous study on infection with *P. berghei* NK65 which did not cause CM (15). These data suggest that MyD88, but not TRIF, is involved in CM symptoms and subsequent death, whereas neither MyD88 nor TRIF is involved in controlling parasitemia or the resultant anemia.

MyD88-dependent parasite sequestration and hemozoin load in the brain

We investigated the mechanisms involved in the pathogenesis of MyD88-dependent CM. Since brain-specific immunopathological changes have been shown to play a critical role in CM development (4, 5, 32), we examined the effects of MyD88 and TRIF on immunopathological changes in the brains of mice 6 days after infection, at which most WT mice begin to develop characteristic symptoms of CM. Histological examination of brain sections revealed that WT mice from a B6 or B6.129 background, as well as TRIF-deficient mice, showed typical vascular occlusion with parasitized erythrocytes as well as leukocytes and microvascular destruction including endothelial cell detachment (Fig. 2A, b and c). However, these characteristic pathological changes were absent in MyD88- but not in TRIF-deficient mice, suggesting that a MyD88-dependent immune response may play a role in the brain pathogenesis of CM (Fig. 2A, d and e, respectively).

We have previously demonstrated that hemozoin, a malaria metabolite during the red blood cell stage, activates the innate immune system via TLR9 and MyD88 (17). To investigate whether hemozoin is involved in the pathogenesis of CM, we attempted to visualize hemozoin clusters in HE-stained brain sections. However, we found that when the sections were stained with Prussian blue, visualization was easier due to faint red staining of the background (Fig. 2B). We counted hemozoin clusters in 25 microvessels per group (*n* = 3 or 4) by light microscopy, and found that hemozoin accumulation was significantly reduced in MyD88-deficient brains compared with that in WT brains at day 6 (Fig. 2C, *P* < 0.001 by Mann–Whitney *U*-test), in spite of comparable systemic parasitemia levels (Fig. 1A).

In addition, we noticed that there was hemozoin residue in the tissues, outside the blood vessels (data not shown). It is

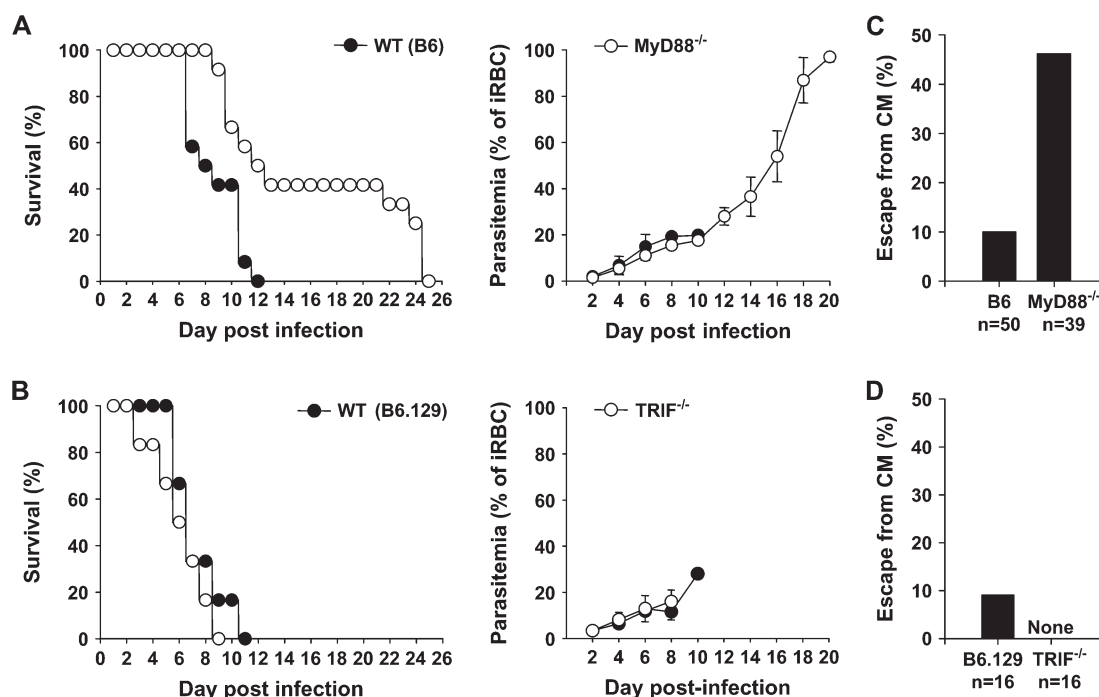


Fig. 1. MyD88- but not TRIF-deficient mice have increased resistance to CM. MyD88^{-/-} and TRIF^{-/-} mice and their WT controls were infected intra-peritoneally with 10⁶ iRBCs of PbA strain. The percentage survival and parasitemia of (A) WT (B6, closed circles) and MyD88-deficient (MyD88^{-/-}, open circles) mice ($n = 12$ for each group) and (B) WT (B6.129, closed circles) and TRIF-deficient (TRIF^{-/-}, open circles) mice ($n = 6$ for each group, littermates) after infection. Survival was monitored daily. Parasitemia was assessed by Giemsa-stained blood smears every other day (mean parasitemia \pm SE). Data shown here are representative of three (B) to six (A) different experiments ($P = 0.003$ for the percentage survival curve of WT versus MyD88^{-/-} mice; $P = 0.327$ for those of WT versus TRIF^{-/-} mice by log rank test). (C) Total escape from CM in MyD88^{-/-} mice until day 12 after infection. Ten percent of WT (B6) mice ($n = 50$) escaped from CM versus 46.15% of MyD88^{-/-} mice ($n = 39$). (D) Total escape from CM in TRIF^{-/-} mice until day 12 after infection. In all, 9.1% of WT (B6.129) mice ($n = 16$) escaped from CM versus 0% of TRIF^{-/-} mice ($n = 16$). 'None' implies that no TRIF^{-/-} mice could survive.

possible that destruction of the blood-brain barrier might allow parasites or hemozoin itself to enter the brain tissue to activate residual microglia cells. Indeed, microglial cell activation during CM has previously been implicated (33), which prompted us to evaluate whether microglia cells, macrophage-like cells in the brain, can be directly activated by hemozoin or crude extract of iRBCs. We stimulated BV-2 cells (26) (a murine microglia cell line expressing TLR9 mRNA (34)) with PbA crude extract and hemozoin for 24 h (Supplementary Figure 1A and B, available at *International Immunology* Online). RT-PCR analysis showed activation by hemozoin or PbA crude extract in BV-2 cells to up-regulate mRNA expression of acute inflammatory response genes such as *Lipocalin 2*, *MIP-1 α* and *IL-6*. We used CpG ODN 1555 as a control (26). Taken together, these data suggest that microglial cell line can respond to hemozoin and PbA crude extract.

Role of MyD88 and TRIF in the immunopathological changes in the brain during PbA infection

In order to comprehensively analyze and identify the genes involved in MyD88-dependent, brain-specific molecular events during CM, we obtained brains from WT mice or MyD88- or TRIF-deficient mice at day 6 after PbA infection, and examined their mRNA expression profiles by DNA microarray analysis. We compared 'fold increases' of mRNA ex-

pression in PbA-infected brain tissue over those in uninfected tissue, which were then compared with those of WT mice (B6 or B6.129) and MyD88- and TRIF-deficient mice. A cut-off value was determined as a 5-fold change in infected brains over that of uninfected WT mice. Genes that showed a <2-fold change between WT and mutant mice were determined as 'independent', whereas those with a >2-fold change were determined as 'dependent'. Accordingly, the transcriptional responses to PbA infection were divided into three categories: genes that are regulated solely by MyD88, by either MyD88 or TRIF or solely by TRIF (Table 1, Supplementary Tables 1 and 2, available at *International Immunology* Online).

Among the genes up-regulated by PbA infection in a MyD88-dependent manner, we noticed that the up-regulation of genes related to TLR-activated microglia cells, such as G-protein-coupled receptor *mFpr-2*, as well as chemokines such as *Ccl3* and *Ccl9*, were also MyD88 dependent, implying that residual microglia or migrated macrophages may also be involved in MyD88-dependent up-regulation of these genes. We found that the genes related to severe malaria, such as *Lipocalin 2* (24p3) (35) and *Haptoglobin* (*Hp*), genes associated with cerebral ischemia, such as *C4b* (complement component 4B), *C1qb*, *Klk7* (Kallikrein 7) and *S3-12* (plasma membrane associated protein) and stress response genes, such as *Atf3*, were up-regulated in the brain in a MyD88-dependent manner.

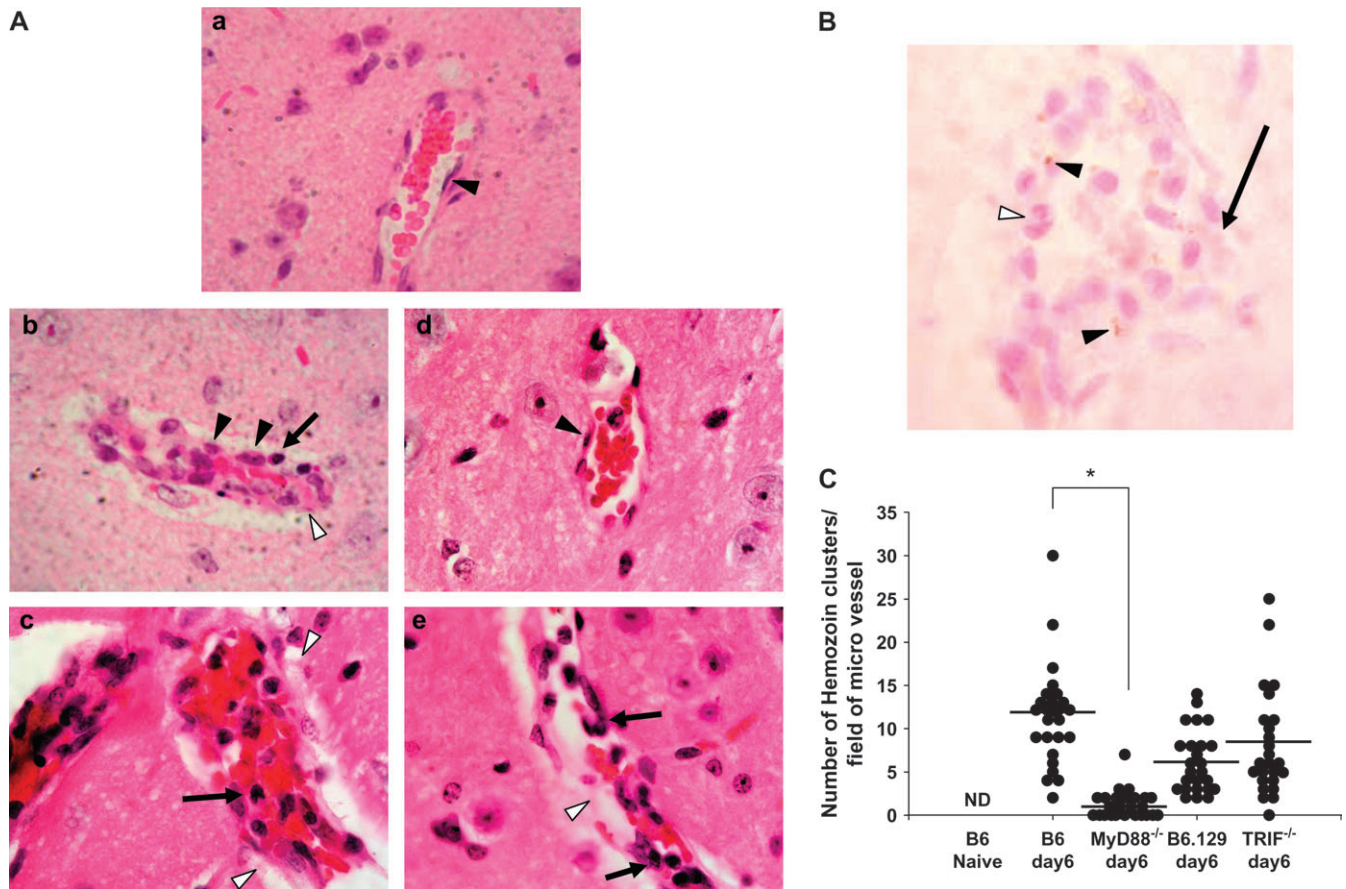


Fig. 2. PbA-infected MyD88-deficient mouse brain displayed a marked decrease in histopathological changes and brain hemozoin load. MyD88^{-/-} and TRIF^{-/-} mice and their WT controls were infected intra-peritoneally with 10^6 RBCs infected with PbA. (A) Histological analysis of brain sections of MyD88^{-/-} and TRIF^{-/-} mice and their WT controls 6 days after PbA infection. Brains were removed and fixed for histological examination. Representative sections from areas around the blood vessels of cerebrum with HE staining are shown ($n = 3$ per group). (a) Normal uninfected mouse brain showing a healthy blood vessel with normal architecture. Endothelial cells (closed triangle, magnification $\times 1000$). (b, c and e) Sections of an infected WT (B6) (b), B6.129 (c) and TRIF^{-/-} (e) mice brains showing severe destruction of endothelial cells (open triangles), sequestration of iRBC (closed triangles) and mononuclear cell infiltration (black arrows, magnification $\times 1000$). (d) Section of an infected MyD88^{-/-} mouse brain showing mostly intact endothelial cells (closed triangle, magnification $\times 1000$) and non-destructed blood vessel. (B) Tissue sections were stained with Prussian blue, and hemozoin clusters were counted by light microscopy. WT brain stained with Prussian blue is shown. Note that shown is a disrupted vessel, with a destruction of endothelial cells (black arrows), and infiltrated mononuclear cells (open triangle) that a counterstaining with nuclear red solution shows very faint staining, but clear visualization of dark brown hemozoin clusters (closed triangle, magnification $\times 1000$). (C) Hemozoin clusters in infiltrated brain vessels were counted in 25 microscopic fields. MyD88^{-/-} mouse brains had significantly lower numbers of hemozoin clusters in each area counted ($P < 0.001$, Mann-Whitney U-test, $n = 3$ or 4 per group). ND represents not detected in uninfected naive mice.

We also noted that the genes which are (i) associated with cytotoxicity, such as *Gzmb* (granzyme B) and *Pdcd1lg1* (programmed cell death 1 ligand 1, also called B7-H1 or CD274); (ii) related to lymphocyte recruitment, such as *Ccl3*, *Ccl9* and *Ccr5*; (iii) IFN (type-I and/or -II) inducible, such as *Vig1*, *Oasl2*, *Tap-1*, *Ifi44*, *Ifi3*, *Ifi35*, *Isg15*, *Irf7*, *Irf9*, *Usp18*, *Ifi1* (LRG-47), *Stat1*, *Mx1*, *Mda5*, *Ppicap* (lectin, also called CyCAP) and *Zfp36* and (iv) expressed in T cells and NK cells, such as *Ms4a4b* (also called *Chandra*) (36), *schlafen 1* and *schlafen 2*. These data suggest that type-I or -II IFN-producing immune cells such as T cells, DCs and/or NK cells may be involved in the up-regulation of such genes in the brain during PbA infection.

Some of the up-regulated genes that are dependent on either MyD88 or TRIF include type-II IFN-inducible genes

such as *Lmp7*, *Ubiquitin D (Ubd)*, *H-2Kd*, *Ifi205*, *Gbp2* and *Ifi47* and GTPases and chemokines such as *Ccl5*, *Cxcl10*, *Cxcl9*, *Cxcl16* and *Ccl21a* indicate that there is, in fact, TRIF-dependent, possibly TLR3- and/or TLR4-mediated, innate immune recognition during PbA infection (Supplementary Table 1, available at *International Immunology Online*).

To confirm the results obtained by DNA microarray analysis, some of the gene expression was monitored by RT-PCR in the brain tissues at day 6 after PbA infection. Significant up-regulation of *Granzyme B*, *Lipocalin 2* and *Ccl3* mRNA expression was observed in a MyD88-dependent manner (Fig. 3, $*P < 0.05$ by Student's *t*-test). The results obtained by DNA microarray analysis revealed novel genes that were up-regulated in a MyD88-dependent manner, suggesting their critical role in CM pathogenesis. Importantly, MyD88-dependent

Table 1. Gene expression profiles in brains of MyD88- and TRIF-deficient mice on day 6 after PbA infection

WT (B6) ^a	MyD88 ^{-/-a}	WT (B6.129) ^a	TRIF ^{-/-a}	Gene product (symbol)	GenBank accession number
Genes that require solely MyD88 (MyD88 dependent) ^b					
280	49	155	91	Membrane-spanning 4-domains, subfamily A, member 4B (<i>Ms4a4b</i>)	BB199001
250	70	75	101	Granzyme B (<i>Gzmb</i>)	NM_013542.1
80	5	70	333	Lipocalin 2 (<i>24p3</i>)	X14607.1
60	0.5	23.75	22	Small inducible cytokine A3 (<i>Scya3</i>) (<i>CCL3</i> ; <i>MIP 1α</i>)	NM_011337.1
55.4	7.9	15.2	71	Schlafen 1 (<i>Slfn1</i>)	NM_011407.1
44	2.6	58	50	ESTs	BB239429
40	15	4.1	20.2	Activating transcription factor 3 (<i>Atf3</i>)	BC019946.1
38	5.3	25.8	40.7	Interferon-induced protein with tetratricopeptide repeats 1 (<i>Ifit1</i>)	NM_008331.1
37.4	2.3	6.7	5.4	Leucine-rich alpha-2-glycoprotein (<i>Lrg</i> -pending)	NM_029796.1
36	1.9	15	16	Haptoglobin (<i>Hp</i>)	NM_017370.1
34.7	7.7	21.7	26	Viral hemorrhagic septicemia virus (VHSV)-induced gene 1 (<i>Vig1</i>)	NM_021384.1
30.8	4.7	45	25	2-5 oligoadenylate synthetase-like 2 (<i>Oasl2</i>)	BQ033138
30.2	3.7	22.6	13.7	transporter 1, ATP-binding cassette, sub-family B (<i>MDR/TAP</i> also called <i>Tap-1</i>)	BC024897.1
28.4	7	18.6	10.5	Programmed cell death 1 ligand 1 (<i>Pdcd11</i> -pending)	NM_021893.1
28	4.5	16.6	14.4	Interferon-induced protein 44 (<i>Ifi44</i>)	NM_133871.1
25.8	1	52	35.7	Kallikrein 7 (<i>Klk7</i>)	NM_011872.1
25.3	1.9	6.2	4.7	Eukaryotic translation initiation factor 2-alpha kinase 2 (<i>Eif2ak2</i>)	AV328340
24.8	3.7	19	17	Interferon-stimulated protein (15 kDa) (<i>Isg15</i>)	AK019325.1
24.2	3.5	15	27.7	ESTs	BB132493
23.9	4.6	28	17.8	28-kDa interferon alpha responsive protein (<i>5830458K16Rik</i>)	NM_023386.1
22.4	0.7	7.2	8.4	Interleukin 1 receptor, type II (<i>Il1r2</i>)	NM_010555.1
21.1	7.8	22.4	35.7	Ubiquitin-specific protease 18 (<i>Usp18</i>)	NM_011909.1
20.2	1.7	5.3	13.6	Plasma membrane-associated protein, S3-12 (<i>S3-12</i> -pending)	NM_020568.1
19	6.7	11.3	7.6	Guanylate nucleotide-binding protein 3 (<i>Gbp3</i>)	NM_018734.1
17.2	3.5	25	10.5	Interferon-inducible protein 1 (<i>Ifi1</i> also called <i>LRG-47</i>)	NM_008326.1
17.1	2.7	12	10.4	Fc fragment of IgG, low affinity IIIa, receptor	BC027310.1
17	4.5	15.7	19	Interferon-induced protein with tetratricopeptide repeats 3 (<i>Ifit3</i>)	NM_010501.1
16.5	4	13.4	13	Interferon regulatory factor 7 (<i>Irf7</i>)	NM_016850.1
16	1.8	4.8	6.65	Formyl peptide receptor, related sequence 2 (<i>Fpr-rs2</i> also called <i>Fpr-2</i>)	NM_008039.1
15.8	2.2	7.5	14.2	Histocompatibility 2, class II antigen A, beta 1 (<i>H2-Bf</i>)	M15848.1
15.7	2.5	11.7	16.4	Membrane-spanning 4-domains, subfamily A, member 9 (<i>Ms4a9</i> also called <i>Ms4a4c</i>)	NM_022429.1
15.6	2.1	14	17	Histocompatibility 2, complement component factor B (<i>H2-Bf</i>)	NM_008198.1
14.8	3.5	12.4	12.6	Peptidylprolyl isomerase C-associated protein (<i>Ppicap</i> also called <i>CyCAP</i>)	NM_011150.1
14.4	2	12	12	Cyclin-dependent kinase inhibitor 1A (<i>P21</i>) (<i>Cdkn1a</i>)	NM_007669.1
13.4	2.4	14.7	8	Interferon-induced protein 35 (<i>Ifi35</i>)	AW986054
11.3	2.3	10.9	5.6	Histocompatibility 2, T region locus 23 (<i>H2-T23</i>)	NM_010398.1
11.3	0.8	5.5	3	Chemokine (C-C) receptor 1 (<i>Cmkbr1</i>)	BC011092.1
11.2	1.5	12.1	10.2	Schlafen 2 (<i>Slfn2</i>)	NM_011408.1
11	0.8	5	4	S100 calcium-binding protein A8 (<i>calgranulin A</i>) (<i>S100a8</i>)	NM_013650.1
11	1.3	2.5	2.2	Glucocorticoid-regulated inflammatory prostaglandin synthase (<i>griPGHS</i>)	M88242.1
10.2	2.4	7.1	6.3	Complement component 4 (<i>C4</i>)	NM_009780.1
10.1	2.3	10.3	10.6	Signal transducer and activator of transcription 1 (<i>Stat1</i>)	BM239586
10	3.9	5.5	4	Fibrinogenangiopoietin-related protein (<i>Angptl4</i>)	NM_020581.1
9.8	0.8	3.8	2.2	CD14 antigen (<i>Cd14</i>)	NM_009841.1
9.5	2	4.6	8.8	F-box protein 39 (<i>Fbxo39</i>)	BB645745
9.2	1.2	8.8	4.8	Apolipoprotein D (<i>Apod</i>)	AV332635
9	2.75	14	8.3	Tripartite motif protein 30 (<i>Trim30Rpt1</i>)	BM240719

Table continues

Table 1. Continued

WT (B6) ^a	MyD88 ^{-/-a}	WT (B6.129) ^a	TRIF ^{-/-a}	Gene product (symbol)	GenBank accession number
8.7	2	7	7.4	<i>Paired-Ig-like receptor A6 (Pira6)</i>	NM_011093.1
8.6	0.8	2.2	1.2	<i>Thrombospondin 1 (THBS1)</i>	AV026492
8.3	2.5	7.5	9.2	<i>Lectin, galactose-binding, soluble 9 (Lgals9)</i>	NM_010708.1
8.3	3.6	4	3.5	<i>Interferon consensus sequence-binding protein (Icsbp)</i>	BG069095
8	2.4	22.3	21.8	<i>Similar to interferon activated gene 203</i>	BM241008
7.5	1.4	7.4	4.8	<i>Integrin beta 2 (Itgb2)</i>	NM_008404.1
7.3	0.8	6.3	4.6	<i>Cathepsin C (Ctsc)</i>	NM_009982.1
7.1	2.2	8.8	8.1	<i>Interferon-dependent positive acting transcription factor 3 gamma (Isgf3g also called Irf9)</i>	NM_008394.1
7.1	1.7	9.5	7.3	<i>Serum amyloid A 3 (SAA3)</i>	NM_011315.1
6.8	1	3.8	2.7	<i>Zinc finger protein 36 (Zfp36 also called Tis11)</i>	X14678.1
5.9	2.4	8.5	11.4	<i>Interferon-induced protein with tetratricopeptide repeats 2 (Ifit2)</i>	NM_008332.1
5.85	2.4	11.9	6.4	<i>Histocompatibility 2, D region locus 1 (H2-D1)</i>	NM_010380.1
5.8	1.8	6.2	23	<i>Mx1 protein (Mx1)</i>	M21039.1
5.5	0.7	5.45	3.5	<i>FK506-binding protein 5 (51 kDa) (Fkbp5)</i>	BC015260.1
5.48	0.9	5	2.6	<i>Metallothionein 2 (Mt2)</i>	AA796766
5.43	1.6	4.28	2.5	<i>Interferon regulatory factor 1 (Irf1)</i>	NM_008390.1
5.3	0.6	3.3	3.4	<i>Small inducible cytokine A9 (Scya9) (CCL9)</i>	NM_011338.1
5.2	2.5	6.8	8.3	<i>Mda5 (Ifih1 also called Helicard)</i>	AY075132.1
5.1	0.6	3.8	2	<i>CD86 antigen (CD86)</i>	AF065897.1
5	0.6	2.6	2.9	<i>C-C chemokine receptor 5 (CCR5)</i>	D83648.1
3.7	1.4	5	4.75	<i>Interferon-stimulated protein (20 kDa) (Isg20)</i>	BC022751.1
3.25	1	7	3.6	<i>Small inducible cytokine A4 (ScyA4) (CCL4 also called MIP-1β)</i>	AF128218.1

^aFold increase in mRNA expression in PbA-infected brain tissue compared with that in uninfected brain tissue. ^bGenes in which changes were <2-fold between WT and mutant mice were classified as 'independent', whereas those with a >2-fold difference were classified as 'dependent'. A cut-off value was determined as a 5-fold change in the infected brains compared with those in uninfected WT mice.

genes, including those coding for chemokines related to lymphocyte recruitment, and lymphocyte-related genes, some of which have been reported as critical for CM pathogenesis (12), prompted us to examine the role of MyD88 in recruitment of lymphocytes during CM pathogenesis.

MyD88-dependent recruitment of CCR5⁺, CD8⁺ T cells and CD11c⁺ DCs, including B220⁺, NK1.1⁺ cells, into PbA-infected mouse brain

It has been shown that recruitment and activation of T cells in the brain during PbA infection play a critical role in CM pathogenesis (37, 38). Based on the brain mRNA expression profile in PbA-infected mice, we examined whether such T cell recruitment occurs and it is controlled by MyD88. Brain cells were isolated from WT or MyD88-deficient mice at 6 days after PbA infection, and analyzed for the number and type of cells by flow cytometry. Similar numbers of mononuclear cells were recovered from all groups of brains (uninfected naive mice contained $14.2 \times 10^6 \pm 4.7 \times 10^6$ cells per brain, WT mice at day 6 of infection contained $14.9 \times 10^6 \pm 8 \times 10^6$ cells per brain and MyD88^{-/-} mice at day 6 of infection contained $10.2 \times 10^6 \pm 1 \times 10^6$ cells per brain, $n = 3-6$ mice per group). Large numbers of Thy1.2⁺ and TCRβ⁺ T cells were observed among cells isolated from the brain at 6 days after infection, while almost no T cells were stained in naive brains suggesting negligible contamination of the cells from the blood flow (Fig. 4A). More than 70% of

these T cells in the infected WT brain were CD8 positive, and the remainder were CD4 positive (Fig. 4A). These CD8⁺ T cells infiltrating the brain also expressed CCR5, whose mRNA was up-regulated in DNA microarray analysis (Fig. 4A and Table 1). Of note, CCL3 (also named MIP-1α), the ligand for CCR5, was also highly up-regulated in the infected brain (Fig. 3 and Table 1). In sharp contrast, the brains of MyD88-deficient mice with no CM symptoms had dramatically fewer CCR5⁺, CD8⁺ T cells (Fig. 4A). As CCL3 was highly up-regulated in the brain, these results suggest that CCR5⁺, CD8⁺ T cells may be recruited to the brain via MyD88-dependent up-regulation of CCL3.

We also found that CD11c⁺ DCs, but not B220⁺ B cells, were increased in number in infected brains in a MyD88-dependent manner (Fig. 4B). Among those CD11c⁺ cells increased, we found that CD11c⁺ and NK1.1⁺ cells were also increased in a MyD88-dependent manner, all of which were CD11c⁺ and B220 dim (Fig. 4B), which displayed identical staining pattern to those identified as hybrid type cells for DCs and NK cells namely IFN-producing killer dendritic cells (IKDCs) (type-I and -II) (28, 29) and certain NK cell subsets as previously described (39, 40). These results suggest that MyD88-mediated signaling triggers expression of genes, such as chemokines, including CCL3, resulting in recruitment of CCR5⁺, CD8⁺ T cells, as well as CD11c⁺ DCs, including CD11c⁺, B220⁺ and NK1.1⁺ cells into the brain. It was also shown by DNA microarray analysis and RT-PCR

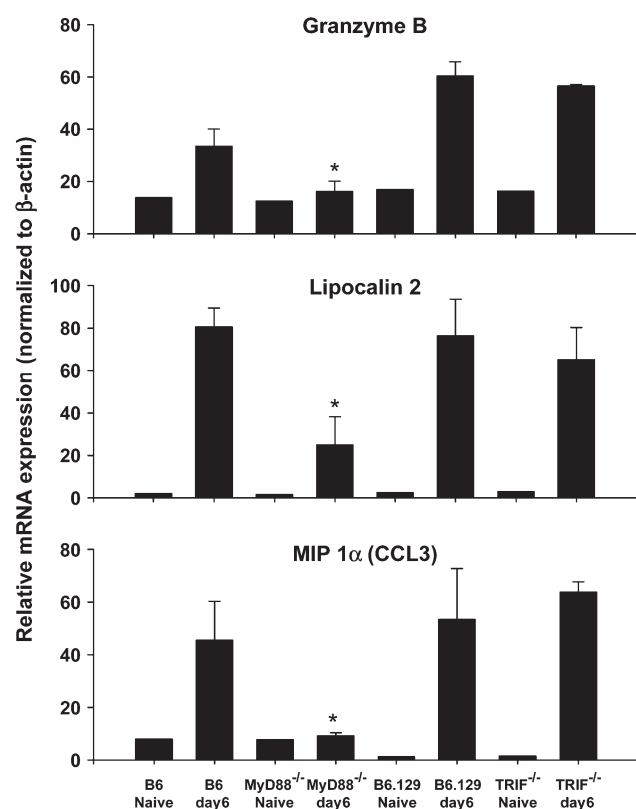


Fig. 3. MyD88-dependent brain mRNA gene expression after PbA infection. MyD88^{-/-} and TRIF^{-/-} mice and their WT controls were infected with 10^6 of PbA iRBCs. Brains were removed 6 days after infection and mRNA expression was analyzed by RT-PCR. Density of the PCR products in ethidium bromide-stained gel was measured by NIH image software. Results (mean \pm SD) are presented as relative units normalized to β -actin, which were obtained from three infected mice per group, and experiments were repeated twice. * $P < 0.05$, infected MyD88^{-/-} or TRIF^{-/-} mice versus infected WT mice (Student's *t*-test).

that genes such as *Ms4a4b* (also called *Chandra*), *granzyme B* and *Ifng*, which are expressed in CD4⁺ and CD8⁺ T cells and NK1.1⁺ cells, and possibly in CD11c⁺, B220⁺ and NK1.1⁺ cells (36), were also highly up-regulated in WT mice brains, but not in those from infected MyD88-deficient mice or uninfected mice (Table 1).

Role of TLRs in the pathogenesis of CM

MyD88 is an essential adaptor molecule for intracellular signaling mediated by most TLRs, as well as IL-1R/IL-18R. Previous reports suggest that IL-18 is up-regulated and involved in protective immunity, rather than lethal complications such as CM in PbA infection (9). *Plasmodium* spp. have been shown to contain ligands for TLR2 and TLR9, such as GPI anchor and hemozoin, respectively (16, 17), which prompted us to examine whether these TLRs are, in fact, involved in the pathogenesis of CM. We infected mice deficient for TLR2, TLR4, TLR5, TLR7 or TLR9 with PbA, and then monitored incidence of CM and survival. Each TLR-deficient mouse was backcrossed to C57BL/6 background at least for eight generations. A significant number of mice lacking TLR2 or TLR9, but not TLR4, TLR5 or TLR7, survived CM and early death be-

tween 6 and 12 days after infection (Fig. 5A–E) ($P < 0.001$ for WT versus TLR2^{-/-} mice; $P = 0.027$ for WT versus TLR9^{-/-} mice; $P > 0.05$ for WT versus TLR4^{-/-}, TLR5^{-/-} or TLR7^{-/-} mice by log rank survival analysis). Overall escape from CM in TLR2- and TLR9-deficient mice until day 12 after infection was significantly higher [10.55% of WT (B6) mice ($n = 28$) versus 55% of TLR2^{-/-} mice ($n = 21$) escaped from CM; 14.7% of WT (B6) mice ($n = 27$) versus 45.8% of TLR9^{-/-} mice ($n = 19$) escaped from CM]. However, TLR4-, TLR5- or TLR7-deficient mice could not escape from CM [10.55% of WT (B6) mice ($n = 28$) versus 0% 16.75% of TLR4^{-/-} mice ($n = 20$) escaped from CM; 14.28% of WT (B6) mice ($n = 14$) versus 0% of TLR5^{-/-} mice ($n = 11$) escaped from CM; 0% of WT (B6) mice ($n = 5$) versus 0% of TLR7^{-/-} mice ($n = 5$) escaped from CM].

Of note, parasitemia was comparable between the WT and each strain of TLR-deficient mice (Fig. 5A and B), which survived CM, while that of MyD88^{-/-} was slightly higher (Fig. 1A). It may be due to compensated innate and adaptive immune responses in TLR2^{-/-} or TLR9^{-/-} mice compared with MyD88^{-/-} mice which lack combined effects of each TLR. While we did not formally exclude the less likely involvement of IL-1 and IL-18, which also require MyD88 for their subsequent functions, these results strongly suggest that TLR2 and TLR9, but not TLR4, TLR5 or TLR7, are involved in the pathogenesis of CM, but not in controlling parasitemia during PbA infection.

Systemic responses and hemozoin load in the brain

Based on the evidence that pro-inflammatory cytokines such as IFN γ , IL-12 and TNF α are associated with the severity of malaria infection including CM (7–9), we investigated the role of MyD88/TLR2/TLR9 pathways on the systemic productions of such cytokines in serum at day 6 after infection. Productions of serum cytokines IFN γ , TNF α and IL-12p40 were significantly dependent on MyD88 ($P < 0.05$ by Mann–Whitney *U*-test) (Fig. 6A). The up-regulation of serum IFN γ , TNF α and IL-12p40 was significantly reduced in MyD88-deficient mice, but not in TRIF- or TLR2-deficient mice. On the other hand, in TLR9^{-/-} mice only TNF α production was TLR9 dependently secreted after PbA infection (Fig. 6A, $P < 0.05$, Mann–Whitney *U*-test). These results suggested that PbA infection causes systemic cytokine productions via MyD88-dependent signaling; however, systemic cytokine productions are not critical for CM development.

We also counted hemozoin clusters in brains of TLR2^{-/-} and TLR9^{-/-} mice after Prussian blue staining and found that hemozoin accumulation was significantly reduced in TLR2- and TLR9-deficient mice brains compared with that in WT brains at day 6 (Fig. 6B, $P < 0.038$ and $P < 0.019$, respectively, by Mann–Whitney *U*-test).

Discussion

In this study, we showed, for the first time, that TLRs and their adaptor molecules play distinct roles in CM pathogenesis. Mice deficient in MyD88, but not in TRIF, displayed significantly less CM-characteristic neurological symptoms, which resulted in significantly reduced mortality. This was supported by histological analysis in which the brains from infected

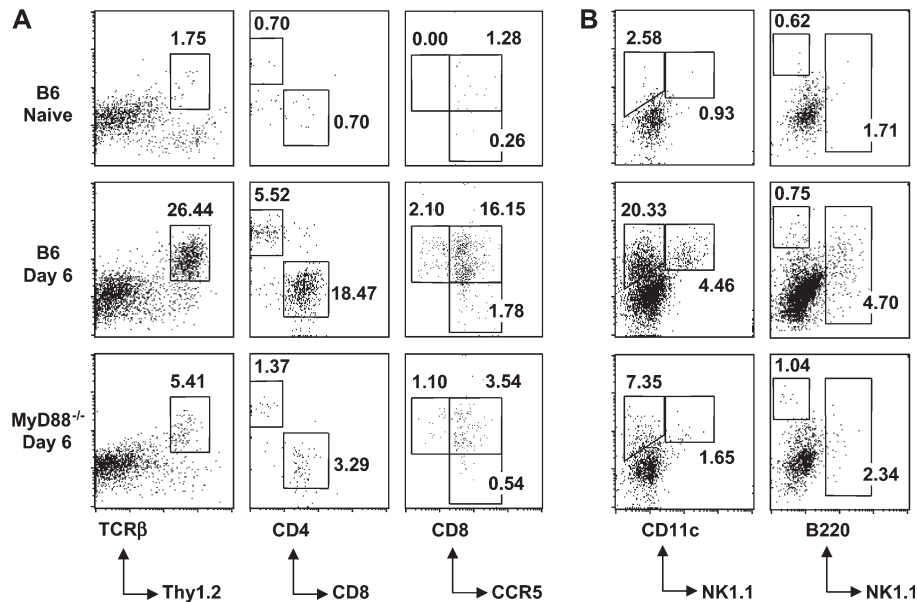


Fig. 4. MyD88-dependent recruitment of CCR5⁺, CD8⁺ T cells and CD11c⁺ cells, including CD11c⁺, B220⁺ and NK1.1⁺ cells, into PbA-infected brain. Brain lymphocytes were isolated from infection-naïve or PbA-infected WT or MyD88^{-/-} mice, and stained with labeled antibodies as described in the experimental procedure. (A) Thy1.2⁺ and TCRβ⁺ T cells (left panel) were stained with antibodies against CD4, CD8 and/or CCR5 (middle and right panels). (B) Cells were stained with anti-CD11c, NK1.1 and/or B220. Numbers represent the percentage of gated cell population in isolated brain lymphocytes. Results are representative of one mouse from each group of three mice. Experiments were repeated three times with similar results.

MyD88-deficient mice displayed reduced endothelial cell damage and sequestration of infected erythrocytes. We could detect hemozoin in infected WT brain blood vessels, as well as in the other brain tissues by microscopy, which was significantly less in MyD88-deficient mice. Moreover, flow cytometry of the recovered lymphocytes from the infected brain suggested that infiltration of T cells, most of which are CCR5⁺, CD8⁺ T cells and CD11c⁺ DCs, including CD11c⁺, B220⁺ and NK1.1 cells, is controlled at least in part by MyD88-dependent signaling. Although not all MyD88-deficient mice survived CM caused by PbA infection, our results strongly suggest that MyD88, but not TRIF, is a key signaling molecule in CM pathogenesis, at least in currently available experimental CM models.

The effect of MyD88 on CM was more obvious in local brain where CM symptom attribute to, rather than systemic control of parasitemia as well as inflammation. Damage of brain blood vessels is a characteristic feature of CM pathogenesis, such as destruction of the endothelial cell layer, sequestration of iRBCs and infiltration of lymphocytes, all of which are dramatically reduced in MyD88-deficient mice compared with either WT or TRIF-deficient mice. We observed parasite sequestration and hemozoin load in these damaged blood vessels in WT infected mice, which was almost diminished in MyD88-deficient mice. Together with the other observation that hemozoin was also detected in brain tissue, and that the microglia cell line was activated by both crude extracts of the iRBCs and hemozoin, but not uninfected RBCs, this suggests that residual microglial cells may be activated by iRBCs that are known to contain TLR ligands, such as GPI and/or hemozoin (16, 17), which have escaped or leaked through the damaged blood-brain barrier.

Comprehensive analysis of MyD88- and/or TRIF-dependent genes in response to PbA infection revealed several important genes that could be involved in CM pathogenesis. MyD88-dependent genes up-regulated by PbA infection included not only those up-regulated by the microglial cell line, but also type-I or -II IFN-inducible genes, T or NK cell-related genes and stress response genes. A recent report identified several genes such as *Gzmb*, *Samhd1*, *Fkbp5*, *Ifit3*, *Igf2r*, *Ctla2a* and *C1qb* which were up-regulated specifically in CM-susceptible mice strains infected with PbA (32). Our results confirmed and further extended these findings; *Gzmb* and *Ifit3* were up-regulated during PbA infection, which was exclusively dependent on MyD88. In addition, we found that *Isg15*, *Mx1*, *Cxcl10* (*IP-10*), *Ccl3* (*MIP-1α*), *Ccr5* and *serum amyloid A* were also up-regulated by PbA infection in a MyD88-dependent manner. Of note, MIP-1α was reported to be up-regulated by hemozoin in macrophages (41). Moreover, *Lipocalin 2* (*24p3*), a gene important for iron metabolism and for resistance against certain bacteria (42) and presumably important marker for severe malaria in humans (35), was highly up-regulated in the brain of PbA-infected mice in a MyD88-dependent manner (Table 1 and Fig. 3). Our preliminary data, however, suggest that mice deficient for *Lipocalin 2* (*24p3*) suffered from and died from CM, as did WT mice (C. Coban, K. J. Ishii, S. Sato and S. Akira, unpublished results).

Among the MyD88-dependent CM-related genes, we noted some that may be involved in innate immune responses (especially type-I and -II IFN-inducible genes) and the recruitment of lymphocytes, such as T cells and/or NK cells. We were initially interested in type-I IFN-inducible genes; however, infection of mice lacking IFNαβR or TBK1 (and/or TNF, which are deficient for TRIF- or TLR-independent type-I IFN

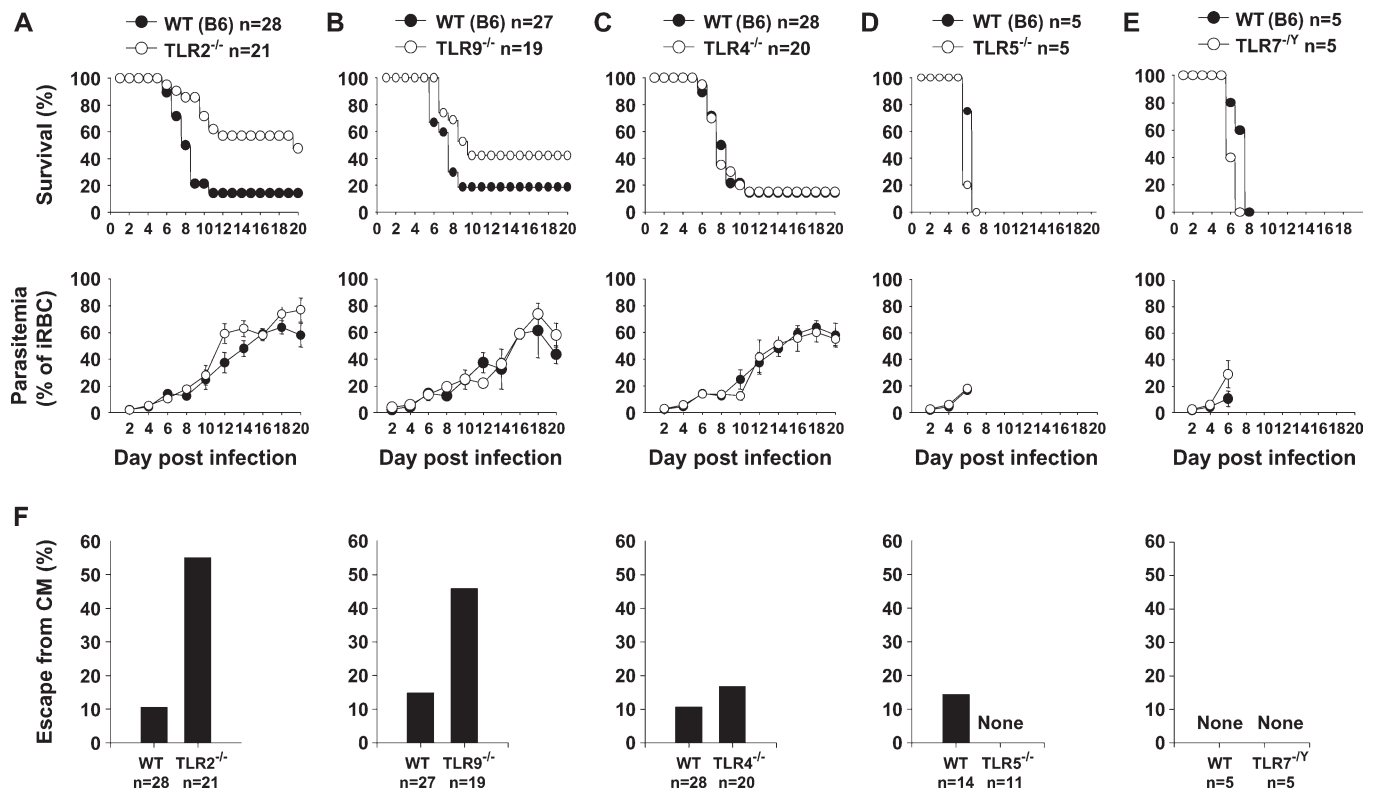


Fig. 5. TLR2^{-/-} and TLR9^{-/-} mice have decreased susceptibility to CM. WT (B6) or mice lacking (A) TLR2, (B) TLR9, (C) TLR4, (D) TLR5 or (E) TLR7 ($n = 28$ for WT and $n = 21$ for TLR2^{-/-}, $n = 27$ for WT and $n = 19$ for TLR9^{-/-}, $n = 28$ for WT and $n = 20$ for TLR4^{-/-}, $n = 5$ for WT and $n = 5$ for TLR5^{-/-} and $n = 5$ for WT and $n = 5$ for TLR7^{-/-}) were infected with 10^6 iRBCs of PbA strain. Survival was monitored daily. Parasitemia was examined from Giemsa-stained blood smears every 2 days (mean parasitemia \pm SE). $P < 0.001$ for the percentage survival curve of WT versus TLR2^{-/-} mice, and $P = 0.027$ for that of WT versus TLR9^{-/-} mice by log rank test. (F) Total escape from CM in TLR-deficient mice until day 12 after infection. In all, 10.55% of WT (B6) mice ($n = 28$) escaped from CM versus 55% of TLR2^{-/-} mice ($n = 21$), 14.7% of WT (B6) mice ($n = 27$) escaped from CM versus 45.8% of TLR9^{-/-} mice ($n = 19$), 10.55% of WT (B6) mice ($n = 28$) escaped from CM versus 16.75% of TLR4^{-/-} mice ($n = 20$), 14.28% of WT (B6) mice ($n = 14$) escaped from CM versus none of TLR5^{-/-} mice ($n = 11$) and none of WT (B6) mice ($n = 5$) escaped from CM versus none of TLR7^{-/-} mice ($n = 5$). 'None' implies that no infected mice could survive.

induction) suffer from CM and died comparably to those of WT mice (C. Coban, K. J. Ishii and S. Akira, unpublished results). Rather, type-II IFN γ may play a more critical role in MyD88-dependent IFN-inducible genes up-regulated during PbA infection, since systemic as well as brain IFN γ but not IFN α were up-regulated in a MyD88-dependent manner (Fig. 6A, and data not shown). In fact, systemic production of IFN γ , TNF α and IL-12p40 was MyD88 dependent, but not TRIF dependent (Fig. 6A). In case of mice lacking TLR2 or TLR9, however, systemic cytokines were not altered except TNF α in TLR9-deficient mice (Fig. 6A), suggesting that systemic cytokines such as IFN γ were compensated between TLR2 and TLR9, although mice lacking TLR2 or TLR9 survived CM significantly better than WT (Fig. 5). It is also conceivable that the systemic cytokine production such as IFN γ may be regulated by TLR-independent, MyD88-dependent signaling pathway, in which IL-1R and IL-18R utilize. We then focused on genes related to T and NK cells which may be the result of their migration into brain controlled by chemokine genes such as *Ccl3*, *Ccl9* and *Ccr5* which were up-regulated in a MyD88-dependent manner (Table 1 and Fig. 3). In fact, we found that both CD4⁺ and CCR5⁺, CD8⁺ T cells and CD11c⁺ DCs including CD11c⁺, B220⁺ and NK1.1⁺ cells infiltrated into

the brain after PbA infection, which was clearly MyD88 dependent. The cells positive for CD11c, B220 and NK1.1 were with identical staining pattern of newly described IKDCs (28, 29) and certain subsets of NK cells expressing either CD11c or B220 (39, 40), suggesting that they may possess cytotoxic ability via *granzyme*. In addition, we found that certain chemokines were highly up-regulated in a MyD88-dependent manner; CCL3 and CCL4 are known to recruit CCR5-positive cells, including T cells, macrophages and DCs. In agreement with previous reports showing that perforin-deficient C57Bl/6 mice (11, 43, 44) and CCR5-deficient mice (12) which lack their killing and recruiting functions, respectively, display increased resistance to CM, we conclude that the MyD88-dependent recruitment of T cells, DCs and cells expressing both DC and NK markers, possibly via chemokine productions in the brain, may play a critical role in CM pathogenesis.

Results obtained in similar experiments using various TLR-deficient mice suggest that TLR2- and/or TLR9-mediated, MyD88-dependent innate immune cascades may play a critical role in the pathogenesis of CM. This coincides with recent evidence that GPI and hemozoin are found to be agonists for TLR2 and TLR9, respectively (16, 17). TLR2 and TLR9 have been shown to co-operate for protective immune responses

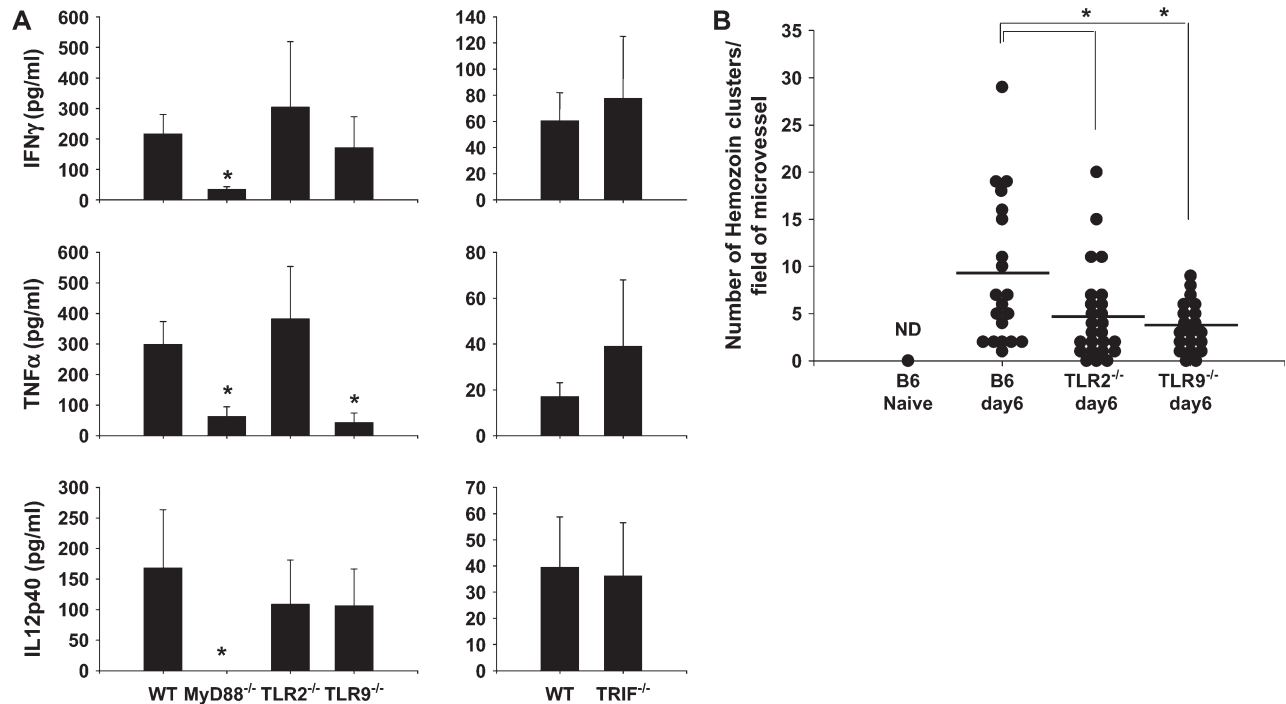


Fig. 6. Systemic cytokine responses and brain hemozoin load after PbA infection. (A) MyD88^{-/-}, TRIF^{-/-}, TLR2^{-/-} and TLR9^{-/-} mice and their WT controls were infected with 10⁶ of PbA iRBCs. Serum levels of IFN γ , TNF α and IL-12p40 at day 6 after infection with PbA were measured by ELISA. Results (mean \pm SE) are from three different experiments that cytokine levels were measured at the same time ($n = 10$ –25 mice per group). * $P = 0.02$ for IFN γ of MyD88^{-/-} versus WT mice, * $P = 0.005$ for TNF α of MyD88^{-/-} versus WT mice * $P = 0.002$ for TLR9^{-/-} versus WT mice and * $P < 0.001$ for IL-12p40 of MyD88^{-/-} versus WT mice (Mann–Whitney U -test). (B) Brain tissue sections were stained with Prussian blue, and hemozoin clusters in infiltrated brain vessels were counted in 20–25 microscopic fields by light microscopy. TLR2^{-/-} and TLR9^{-/-} mouse brains had significantly lower numbers of hemozoin clusters in each area counted ($P < 0.038$ and $P < 0.019$, respectively, Mann–Whitney U -test, $n = 2$ or 3 per group). ND represents not detected in uninfected naive mice.

against various infectious organisms including *Mycobacterium tuberculosis* (45), while TLR9 and TLR2 have been shown to play a reciprocal role in protective immunity and pathology during *Herpes simplex virus* infection, respectively (46). In the case of PbA infection, an absence of TLR2 or TLR9 increases resistance to CM-related mortality but not parasitemia, suggesting that these two TLRs play a critical role in the pathogenesis, and not in protective immunity. A similar strategy was observed for West Nile Virus to utilize TLR3 to facilitate infection in the brain (47). However, further investigation may be needed to clarify whether these TLRs play similar roles in the case of the other *Plasmodium* species such as *Plasmodium yoelii* or *chabaudi*.

In contrast to TLR2 and TLR9, the other TLRs utilizing MyD88 as an essential adaptor, such as TLR5 and TLR7, as well as TLR4, which utilize both MyD88 and TRIF, were not involved in CM pathogenesis and its resultant mortality (Fig. 5). It is of note that, although TRIF-deficient mice die in the same way as WT mice, some genes up-regulated by PbA infection were TRIF dependent (Supplementary Table 2, available at *International Immunology* Online). These results suggest that there are TRIF-dependent innate immune responses during PbA infection, and therefore, it is interesting to investigate the role of TRIF-dependent recognition in the immune response to PbA infection and to identify as yet unknown ligands. Receptors for IL-1 and IL-18 are also known to utilize MyD88 for their sequential signaling; however, previous reports have

suggested that both IL-1 and IL-18 are not involved in CM pathogenesis (8, 9). While specific cell types, by which TLR2 and/or TLR9 mediate MyD88-dependent innate and adaptive immune cascades leading to CM, have not been formally identified, the present study will hopefully help in discerning the complex role of innate immunity in CM pathogenesis.

Overall, the results presented in the current work suggest that innate immune responses via TLR2-, TLR9- and MyD88-dependent pathway are critically involved in the pathogenesis of CM, in which local rather than systemic pro-inflammatory responses plus adaptive immune responses particularly in brain tissue lead to infiltration of CD8 T cells, DCs including those with NK cell marker into brain, and up-regulation of variety of genes related to CM, resulting in the pathogenic changes as we described above. A few information are available whether TLRs or their signaling pathways are involved in human malaria infection; TLR4 frequent single-nucleotide polymorphism (SNP), Asp299Gly, is associated with severe malaria and risk of maternal malaria, whereas TLR9 SNP, T-1486C increased the risk of maternal malaria, but was not associated with severe malaria (48, 49). Although relevance of murine experimental CM models to human CM is under debate; however, our findings with the best available model of CM with PbA infection strongly suggest that host innate immune system against malaria and its exploitation by parasites hold a key to further understanding of pathogenesis of human CM.

Supplementary data

Supplementary figure 1 and tables 1 and 2 are available at *International Immunology Online*.

Acknowledgements

We thank Yukiko Fujita for her excellent technical assistance. This study was supported by grants from the Ministry of Education, Culture, Sports, Science and Technology in Japan and from the 21st Century Center of Excellence Program of Japan.

Abbreviations

APC	allophycocyanin
CM	cerebral malaria
DC	dendritic cell
FBS	fetal bovine serum
GPI	glycosyl-phosphatidylinositol
HE	hematoxylin and eosin
IKDC	IFN-producing killer dendritic cell
iRBC	infected RBC
MyD88	myeloid differentiation primary response gene 88
PbA	<i>Plasmodium berghei</i> ANKA
RT	reverse transcription
SNP	single-nucleotide polymorphism
TLR	Toll-like receptor
TNF	tumor necrosis factor
TRIF	TIR domain containing adaptor-inducing IFN-beta
WT	wild type

References

- Aikawa, M. 1988. Human cerebral malaria. *Am. J. Trop. Med. Hyg.* 39:3.
- Miller, L. H., Baruch, D. I., Marsh, K. and Doumbo, O. K. 2002. The pathogenic basis of malaria. *Nature* 415:673.
- Idro, R., Jenkins, N. E. and Newton, C. R. 2005. Pathogenesis, clinical features, and neurological outcome of cerebral malaria. *Lancet Neurol.* 4:827.
- Good, M. F., Xu, H., Wykes, M. and Engwerda, C. R. 2005. Development and regulation of cell-mediated immune responses to the blood stages of malaria: implications for vaccine research. *Annu. Rev. Immunol.* 23:69.
- Schofield, L. and Grau, G. E. 2005. Immunological processes in malaria pathogenesis. *Nat. Rev. Immunol.* 5:722.
- Engwerda, C., Belnoue, E., Gruner, A. C. and Renia, L. 2005. Experimental models of cerebral malaria. *Curr. Top. Microbiol. Immunol.* 297:103.
- Hunt, N. H. and Grau, G. E. 2003. Cytokines: accelerators and brakes in the pathogenesis of cerebral malaria. *Trends Immunol.* 24:491.
- Curfs, J. H., van der Meer, J. W., Sauerwein, R. W. and Eling, W. M. 1990. Low dosages of interleukin 1 protect mice against lethal cerebral malaria. *J. Exp. Med.* 172:1287.
- Singh, R. P., Kashiwamura, S., Rao, P., Okamura, H., Mukherjee, A. and Chauhan, V. S. 2002. The role of IL-18 in blood-stage immunity against murine malaria *Plasmodium yoelii* 265 and *Plasmodium berghei* ANKA. *J. Immunol.* 168:4674.
- Hansen, D. S., Siomos, M. A., Buckingham, L., Scalzo, A. A. and Schofield, L. 2003. Regulation of murine cerebral malaria pathogenesis by CD1d-restricted NKT cells and the natural killer complex. *Immunity* 18:391.
- Belnoue, E., Kayibanda, M., Vigario, A. M. *et al.* 2002. On the pathogenic role of brain-sequestered alphabeta CD8+ T cells in experimental cerebral malaria. *J. Immunol.* 169:6369.
- Belnoue, E., Kayibanda, M., Deschemin, J. C. *et al.* 2003. CCR5 deficiency decreases susceptibility to experimental cerebral malaria. *Blood* 101:4253.
- Akira, S., Uematsu, S. and Takeuchi, O. 2006. Pathogen recognition and innate immunity. *Cell* 124:783.
- Ishii, K. J., Coban, C. and Akira, S. 2005. Manifold mechanisms of toll-like receptor-ligand recognition. *J. Clin. Immunol.* 25:511.
- Adachi, K., Tsutsui, H., Kashiwamura, S. *et al.* 2001. *Plasmodium berghei* infection in mice induces liver injury by an IL-12- and toll-like receptor/myeloid differentiation factor 88-dependent mechanism. *J. Immunol.* 167:5928.
- Krishnegowda, G., Hajjar, A. M., Zhu, J. *et al.* 2005. Induction of proinflammatory responses in macrophages by the glycosylphosphatidylinositols of *Plasmodium falciparum*: cell signaling receptors, glycosylphosphatidylinositol (GPI) structural requirement, and regulation of GPI activity. *J. Biol. Chem.* 280:8606.
- Coban, C., Ishii, K. J., Kawai, T. *et al.* 2005. Toll-like receptor 9 mediates innate immune activation by the malaria pigment hemozoin. *J. Exp. Med.* 201:19.
- Pichyangkul, S., Yongvanitchit, K., Kum-arb, U. *et al.* 2004. Malaria blood stage parasites activate human plasmacytoid dendritic cells and murine dendritic cells through a Toll-like receptor 9-dependent pathway. *J. Immunol.* 172:4926.
- Adachi, O., Kawai, T., Takeda, K. *et al.* 1998. Targeted disruption of the MyD88 gene results in loss of IL-1- and IL-18-mediated function. *Immunity* 9:143.
- Yamamoto, M., Sato, S., Hemmi, H. *et al.* 2003. Role of adaptor TRIF in the MyD88-independent toll-like receptor signaling pathway. *Science* 301:640.
- Takeuchi, O., Hoshino, K., Kawai, T. *et al.* 1999. Differential roles of TLR2 and TLR4 in recognition of gram-negative and gram-positive bacterial cell wall components. *Immunity* 11:443.
- Hoshino, K., Takeuchi, O., Kawai, T. *et al.* 1999. Cutting edge: Toll-like receptor 4 (TLR4)-deficient mice are hyporesponsive to lipopolysaccharide: evidence for TLR4 as the Lps gene product. *J. Immunol.* 162:3749.
- Hemmi, H., Kaisho, T., Takeuchi, O. *et al.* 2002. Small anti-viral compounds activate immune cells via the TLR7 MyD88-dependent signaling pathway. *Nat. Immunol.* 3:196.
- Hemmi, H., Takeuchi, O., Kawai, T. *et al.* 2000. A Toll-like receptor recognizes bacterial DNA. *Nature* 408:740.
- Uematsu, S., Jang, M. H., Chevrier, N. *et al.* 2006. Detection of pathogenic intestinal bacteria by Toll-like receptor 5 on intestinal CD11c(+) lamina propria cells. *Nat. Immunol.* 7:868.
- Takeshita, S., Takeshita, F., Haddad, D. E., Janabi, N. and Klinman, D. M. 2001. Activation of microglia and astrocytes by CpG oligodeoxynucleotides. *Neuroreport* 12:3029.
- Omer, F. M., De Souza, J. B., Corran, P. H., Sultan, A. A. and Riley, E. M. 2003. Activation of transforming growth factor beta by malaria parasite-derived metalloproteinases and a thrombospondin-like molecule. *J. Exp. Med.* 198:1817.
- Chan, C. W., Crafton, E., Fan, H. N. *et al.* 2006. Interferon-producing killer dendritic cells provide a link between innate and adaptive immunity. *Nat. Med.* 12:207.
- Taieb, J., Chaput, N., Menard, C. *et al.* 2006. A novel dendritic cell subset involved in tumor immunosurveillance. *Nat. Med.* 12:214.
- Ishii, K. J., Coban, C., Kato, H. *et al.* 2006. A Toll-like receptor-independent antiviral response induced by double-stranded B-form DNA. *Nat. Immunol.* 7:40.
- Akira, S. and Takeda, K. 2004. Toll-like receptor signalling. *Nat. Rev. Immunol.* 4:499.
- Delahaye, N. F., Coltel, N., Puthier, D. *et al.* 2006. Gene-expression profiling discriminates between cerebral malaria (CM)-susceptible mice and CM-resistant mice. *J. Infect. Dis.* 193:312.
- Medana, I. M., Hunt, N. H. and Chan-Ling, T. 1997. Early activation of microglia in the pathogenesis of fatal murine cerebral malaria. *Glia* 19:91.
- Dalpe, A. H., Schafer, M. K., Frey, M. *et al.* 2002. Immunostimulatory CpG-DNA activates murine microglia. *J. Immunol.* 168:4854.
- Mohammed, A. O., Elghazali, G., Mohammed, H. B. *et al.* 2003. Human neutrophil lipocalin: a specific marker for neutrophil activation in severe *Plasmodium falciparum* malaria. *Acta Trop* 87:279.
- Xu, H., Williams, M. S. and Spain, L. M. 2006. Patterns of expression, membrane localization, and effects of ectopic expression suggest a function for MS4a4B, a CD20 homolog in Th1 T cells. *Blood* 107:2400.

- 37 Finley, R. W., Mackey, L. J. and Lambert, P. H. 1982. Virulent *P. berghei* malaria: prolonged survival and decreased cerebral pathology in cell-dependent nude mice. *J. Immunol.* 129:2213.
- 38 Bauer, P. R., Van Der Heyde, H. C., Sun, G., Specian, R. D. and Granger, D. N. 2002. Regulation of endothelial cell adhesion molecule expression in an experimental model of cerebral malaria. *Microcirculation* 9:463.
- 39 Laouar, Y., Sutterwala, F. S., Gorelik, L. and Flavell, R. A. 2005. Transforming growth factor-beta controls T helper type 1 cell development through regulation of natural killer cell interferon-gamma. *Nat. Immunol.* 6:600.
- 40 Hayakawa, Y. and Smyth, M. J. 2006. CD27 dissects mature NK cells into two subsets with distinct responsiveness and migratory capacity. *J. Immunol.* 176:1517.
- 41 Jaramillo, M., Godbout, M. and Olivier, M. 2005. Hemozoin induces macrophage chemokine expression through oxidative stress-dependent and -independent mechanisms. *J. Immunol.* 174:475.
- 42 Flo, T. H., Smith, K. D., Sato, S. *et al.* 2004. Lipocalin 2 mediates an innate immune response to bacterial infection by sequestering iron. *Nature* 432:917.
- 43 Nitcheu, J., Bonduelle, O., Combadiere, C. *et al.* 2003. Perforin-independent brain-infiltrating cytotoxic CD8⁺ T lymphocytes mediate experimental cerebral malaria pathogenesis. *J. Immunol.* 170:2221.
- 44 Potter, S., Chan-Ling, T., Ball, H. J. *et al.* 2006. Perforin mediated apoptosis of cerebral microvascular endothelial cells during experimental cerebral malaria. *Int. J. Parasitol.* 36:485.
- 45 Bafica, A., Scanga, C. A., Feng, C. G., Leifer, C., Cheever, A. and Sher, A. 2005. TLR9 regulates Th1 responses and cooperates with TLR2 in mediating optimal resistance to *Mycobacterium tuberculosis*. *J. Exp. Med.* 202:1715.
- 46 Morrison, L. A. 2004. The Toll of herpes simplex virus infection. *Trends Microbiol.* 12:353.
- 47 Wang, T., Town, T., Alexopoulou, L., Anderson, J. F., Fikrig, E. and Flavell, R. A. 2004. Toll-like receptor 3 mediates West Nile virus entry into the brain causing lethal encephalitis. *Nat. Med.* 10:1366.
- 48 Mockenhaupt, F. P., Cramer, J. P., Hamann, L. *et al.* 2006. Toll-like receptor (TLR) polymorphisms in African children: common TLR-4 variants predispose to severe malaria. *Proc. Natl Acad. Sci. USA* 103:177.
- 49 Mockenhaupt, F. P., Hamann, L., von Gaertner, C. *et al.* 2006. Common polymorphisms of toll-like receptors 4 and 9 are associated with the clinical manifestation of malaria during pregnancy. *J. Infect. Dis.* 194:184.